Modulational instability and solitons in nonlocal media with competing nonlinearities

Esbensen, B. K.; Wlotzka, A.; Bache, Morten; Bang, Ole; Krolikowski, W.

Published in:
Physical Review A

Link to article, DOI:
10.1103/PhysRevA.84.053854

Publication date:
2011

Document Version
Publisher's PDF, also known as Version of record

Modulational instability and solitons in nonlocal media with competing nonlinearities

B. K. Esbensen,[1] A. Wlotzka,[2] M. Bache,[1] O. Bang,[1] and W. Krolikowski[3]

[1]*DTU Fotonik, Department of Photonics Engineering, Technical University of Denmark, DK-2800 Kgs. Lyngby, Denmark*

[2]*Department of Physics, Institut für Theoretische Festkörperphysik, University of Karlsruhe, D-76128 Karlsruhe, Germany*

[3]*Laser Physics Centre, Research School of Physics and Engineering, Australian National University, Canberra, Australian Capital Territory 0200, Australia*

(Received 19 October 2011; published 28 November 2011)

We investigate analytically and numerically propagation and spatial localization of light in nonlocal media with competing nonlinearities. In particular, we discuss conditions for the modulational instability of plane waves and formation of spatial solitons. We show that the competing focusing and defocusing nonlinearities enable coexistence of dark or bright spatial solitons in the same medium by varying the intensity of the beam.

DOI: 10.1103/PhysRevA.84.053854 PACS number(s): 42.65.Tg, 03.75.Lm

I. INTRODUCTION

Bright and dark spatial optical solitons, i.e., nondiffracting beams propagating in nonlinear media, are formed thanks to an interplay between diffraction, which tends to spread the beam and the self-induced nonlinear refractive index change of the medium, which focuses the beam. In the stationary regime these two processes are exactly in equilibrium, leading to beam self-trapping and its propagation as a soliton [1,2]. In typical nonlinear media the nonlinear response, i.e., the light-induced refractive index change, is a local function of the light intensity. Recently, there has been growing interest in the so-called nonlocal nonlinear media where the nonlinear response of the medium in a particular location depends on the light intensity in a certain neighborhood of this location [3]. In the most extreme case the degree of nonlocality can be so strong that the resulting nonlinear response is no longer a function of the beam intensity but, rather, its total power [4]. Nonlocal nonlinearities have been identified in a variety of physical systems where the nonlocal response is caused by either transport processes such as heat [5] or ballistic atomic transport [6] and diffusion [7] and charge separation [8] or long-range interactions as in dipolar Bose-Einstein condensates [9–11] or nematic liquid crystals [12–14]. It has also been demonstrated that parametric nonlinear wave interactions, such as second-harmonic generation, is in fact well described by a nonlocal nonlinearity, which has enabled accurate descriptions of quadratic solitons [15], modulational instability [16], and soliton pulse compression [17–19] in quadratic nonlinear materials.

The nonlocality has been shown to have a dramatic impact on formation and properties of solitons. In particular, it may arrest collapse of finite beams [3,20–22] and stabilize complex soliton structures such as vortex [23–25], multipeak, and rotating solitons [26–28]. In addition, the nonlocal character of the nonlinearity has been shown to affect the interaction of solitons by providing attractive force between even remote solitons [4,29–31]. This leads to the attraction of otherwise repelling solitons and the formation of bound states of bright and dark solitons [32–37]. The interplay between nonlocality and partial coherence has been studied in Ref. [38], but in contrast to nonlocality, partial coherence is not able to arrest collapse [39].

The notion of nonlocal nonlinearity has been recently extended to media with the so-called synthetic nonlinearities. Those are media where the nonlinear response is a result of two or more competing processes or effects. The concept of competing nonlinearities has been discussed originally in local Kerr-type nonlinear media with simultaneous presence of cubic and quintic nonlinearities [40] or in quadratic media with second-order and Kerr nonlinearities [41]. As far as the nonlocal media are concerned, a competing nonlinear response occurs naturally in Bose-Einstein condensates with dipolar interactions. It has been demonstrated that such a cold gas of bosons is characterized by the simultaneous presence of local (contact) and nonlocal (dipole-dipole) nonlinear interaction potentials with their relative strengths and signs (repulsive/attractive) controlled by experimental conditions [11,42–44]. Given the nonlocal nature of parametric-wave interactions [15], quadratic media such as, e.g., ferroelectric crystals actually inherently constitute a system of competing nonlinearities as they simultaneously support local (Kerr) and nonlocal ($\chi^{(2)}$) nonlinear responses. Early works have found, for example, that competition between those nonlinearities arrests collapse [45] and stabilizes solitons [46].

Competing nonlinearities can be also realized in nematic liquid crystals where they involve both thermal and orientational nonlinear responses to the light beam [47]. The combination of fast local and slow nonlocal nonlinearities has been recently proposed as a way to create stable optical bullets [48]. Few recent works have analyzed the effect of competing nonlocal nonlinearities on existence and stability of solitons. It has been shown, for instance, that the simultaneous presence of nonlocal nonlinearities of opposite sign leads to stabilization of complex soliton structures which are otherwise unstable in a medium with one type of nonlocal nonlinearity [49–51]. On the other hand, it has been also demonstrated that sometimes competing nonlinearities may destabilize dark soliton states [52] and lead to repulsion of in-phase bright solitons [53].

In this article we study analytically and numerically the modulational instability of plane waves and soliton formation in nonlocal media with competing nonlinearities. In particular, we will explore the interplay between nonlocality and the nonlinearity and its effect on stability of bright and dark solitons. We will also discuss the regime in which the

nonlocal medium simultaneously support bright and dark spatial solitons.

II. MODEL

We will consider propagation of waves (optical beams) with a slowly varying amplitude $u(x,z)$ and corresponding intensity $I = |u(x,z)|^2$ in nonlinear media with an intensity-dependent refractive index change $\Delta n(x,I)$. Here x and z represent transverse and longitudinal coordinates, respectively. Such a situation corresponds, for instance, to propagation of beams in a planar waveguide where the spatial confinement along one of the transverse coordinates is provided by the waveguide structure. The evolution of this one-dimensional beam in a phenomenological model of a nonlinear medium is represented by the following nonlocal nonlinear Schrödinger (NLS) equation:

$$\mathrm{i}\frac{\partial u}{\partial z} + \frac{\partial^2 u}{\partial x^2} + \Delta n u = 0. \tag{1}$$

In the case of two competing nonlocal nonlinearities, the nonlinear refractive index change of the medium can be represented by the following phenomenological model:

$$\begin{aligned}\Delta n(x,I) &= \alpha_1 \Delta n_1(x,I) + \alpha_2 \Delta n_2(x,I) \\ &= \alpha_1 \int R_1(x-x')I(x',z)\,dx' \\ &\quad + \alpha_2 \int R_2(x-x')I(x',z)\,dx',\end{aligned} \tag{2}$$

where α_1 and α_2 represent the strength and sign of the two nonlinear contributions, respectively. In what follows α_1 will be considered positive, corresponding to a self-focusing nonlinearity, while α_2 is negative, corresponding to a self-defocusing nonlinearity. The nonlocal response function $R_{1,2}(x)$ defines the nonlocal character of the nonlinearity. Its width (compared to the spatial extent of the beam) determines the degree of nonlocality. In the limiting case of $R_{1,2}(x) = \delta(x)$, Eq. (4) describes a local medium. On the other hand, in the case of a strong nonlocality, the nonlinearity becomes

$$\Delta n(x,I) = P[(\alpha_1 R_1(x) + \alpha_2 R_2(x)], \tag{3}$$

where $P = \int I(x)dx$ denotes the power of the beam. In this regime, the medium behaves as a linear medium with a refractive index profile determined entirely by the nonlocal response functions. The particular form of the nonlocal response function is dictated by the physics of the process responsible for the nonlocality. In particular, $R_i(x) = \sigma_i^{-1}\exp(-|x|/\sigma_i)$ describes the nonlinear response of the nematic liquid crystals in one transverse dimension [13,14]. Here σ_i $(i = 1,2)$ defines the width of the respective nonlocal response. It turns out that many properties of nonlocal nonlinear waves do not depend on the particular form of the nonlocal response [54]. Thus even a box-shaped response function may be used to provide valuable physical insight into the effect of nonlocality [33,55]. Without loss of generality, in this work we will use the so-called Gaussian nonlocal response function $R_i(x) = 1/\sqrt{\pi}\sigma_i \exp(-|x|^2/\sigma_i^2)$.

III. MODULATIONAL INSTABILITY

Modulational instability (MI) is one of the most fundamental effects associated with wave propagation in nonlinear media. It signifies the exponential growth of a small perturbation of the plane-wave (PW) amplitude during propagation. The gain leads to the generation of side bands which break up the otherwise uniform wave front, and generates localized structures. The presence of modulational instability is closely connected with the existence of soliton solutions to the nonlocal NLS equation. MI may act as a precursor for the formation of bright solitons, whereas dark solitons require modulational stability of the constant intensity background.

The nonlocal NLS equation Eqs. (1) and (4) permits exact plane-wave solutions of the form

$$u(x,z) = A_0 \exp\left[ik_0 x - i\omega_0 z\right], \tag{4}$$

where A_0, k_0, and ω_0 are linked through the nonlinear dispersion relation

$$\omega_0 = k_0^2 - (\alpha_1 + \alpha_2)A_0^2. \tag{5}$$

To investigate the stability of this plane-wave solution we carry out a linear stability analysis following our earlier work [54,56].

We consider a small complex perturbation $a(x,z)$ to the PW solution,

$$u(x,z) = [A_0 + a(x,z)]\exp\left[ik_0 x - \mathrm{i}\omega_0 z\right], \tag{6}$$

where $|a(x,z)| \ll 1$. Inserting this perturbed solution into the nonlocal NLS equation Eq. (1) and linearizing around the unperturbed solution [Eq. (6)] yields

$$i\frac{\partial a}{\partial z} + \frac{\partial^2 a}{\partial x^2} + 2ik_0\frac{\partial a}{\partial x} + 2A_0^2\int_{-\infty}^{\infty} R(x-x')\mathrm{Re}\{a(x')\}dx' = 0. \tag{7}$$

Equation Eq. (5) was used to derive this equation, and, for convenience, we have introduced the full response function of the nonlocal medium

$$R(x) = \alpha_1 R_1(x) + \alpha_2 R_2(x). \tag{8}$$

By decomposing the perturbation into real and imaginary parts and Fourier transforming the resulting system of coupled equations, we find that the perturbation evolves with propagation as $a(x,z) \propto \exp(\lambda z)$ where the so-called growth rate λ is determined by the following relation:

$$\lambda^2 = -k^2 A_0^2\left[\frac{1}{A_0^2}k^2 - 2\tilde{R}(k)\right]. \tag{9}$$

where $\tilde{R}(k)$ is a Fourier transform of the nonlocal response function. Therefore, plane-wave solutions are stable if perturbations at any wave number k do not grow with propagation. This is the case as long as λ is purely imaginary. Physically, modulational stability means that small-amplitude waves can propagate along with the background intense PW, although their propagation parameter λ depends on the PW intensity A_0^2. Since $k^2 A_0^2 > 0$, PW solutions are unstable if

$$\frac{1}{A_0^2}k^2 - 2\tilde{R}(k) < 0. \tag{10}$$

We note that if the response function is real and symmetric, which is the case in the majority of physically relevant situations, then so is its Fourier transform, i.e.,

$$R(\xi) = R^*(\xi) = R(-\xi) \Rightarrow \tilde{R}(k) = \tilde{R}^*(k) = \tilde{R}(-k). \quad (11)$$

Since each of the individual response functions, R_j, is normalized, $\tilde{R}(0) = \alpha_1 + \alpha_2$. If $\alpha_1 > |\alpha_2|$ we will, therefore, always have $2\tilde{R}(k) > k^2/A_0^2$, and, thus, $\lambda^2 > 0$, in a certain band symmetrically centered about the origin for sufficiently small k. Therefore, independent of the details in the behavior of the symmetric response function, we always have long-wave MI in this regime. When $|\alpha_2| > \alpha_1$, the stability properties depend on the exact behavior of the response function. If $\tilde{R}(k) \leqslant 0$ for all $k \in \mathbb{R}$, PW solutions are modulationally stable. On the other hand, if $\tilde{R}(k) > 0$ for $k \in I \subset \mathbb{R}$, PWs will be unstable if the intensity A_0^2 is sufficiently high.

In the case of Gaussian nonlocal response functions the Fourier transform of the full nonlocal response is

$$\tilde{R}(k) = \alpha_1 \exp\left[-\frac{1}{4}k^2\sigma_1^2\right] + \alpha_2 \exp\left[-\frac{1}{4}k^2\sigma_2^2\right]. \quad (12)$$

As pointed out earlier, we always have long-wave MI if $\alpha_1 > |\alpha_2|$. Figure 1(a) shows the function $2\tilde{R}(k)$ together with k^2/A_0^2 for $A_0 = 1$ and $A_0 = 2$. The medium parameters are $\alpha_1 = 2$, $\alpha_2 = -1$, $\sigma_1 = 1$, and $\sigma_2 = 3$. As is evident, for sufficiently small wave numbers $2\tilde{R}(k) > k^2/A_0^2$, and we do have MI. The width of the k band in which $2\tilde{R}(k) > k^2/A_0^2$ increases with increasing intensity.

The MI gain is defined as the positive real part of the eigenvalue λ,

$$g(k) = |\mathrm{Re}\{\lambda\}| = kA_0\left|\mathrm{Re}\left\{\sqrt{2\tilde{R}(k) - \frac{1}{A_0^2}k^2}\right\}\right|. \quad (13)$$

Figure 1(b) shows the gain curves for $A_0 = 2$, $A_0 = 4$, and $A_0 = 6$. In addition to the increase in the MI bandwidth, the maximum gain also increases with increasing intensity.

The graph in Fig. 2(a) shows how the MI gain depends on k and σ_1 for constant $\sigma_2 = 3$ and PW amplitude $A_0 = 1$. As σ_1 increases, the MI bandwidth shrinks and the maximum gain decreases. Thus, increasing the width of the self-focusing response tends to suppress MI. The dependence of the gain on σ_2 for constant $\sigma_1 = 1$ and PW amplitude $A_0 = 1$ is shown in Fig. 2(b). As σ_2 is increased from unity, the maximum gain as well as the MI bandwidth increases. However, for sufficiently large σ_2, the maximum gain stays almost constant when σ_2 is increased further. The observed behavior is due to the fact that when σ_1 (σ_2) is large, $\tilde{R}_1(k)$ ($\tilde{R}_2(k)$) is so narrow that the MI properties are primarily determined by $\tilde{R}_2(k)$ ($\tilde{R}_1(k)$).

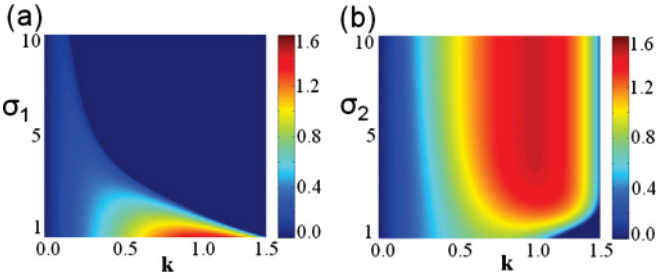

FIG. 2. (Color online) MI gain as function of k and σ_1 (a) and σ_2 (b) for $\alpha_1 > |\alpha_2|$ and $A_0 = 1$. The medium parameters are $\alpha_1 = 2$, $\alpha_2 = -1$ and $\sigma_2 = 3$ (a) and $\sigma_1 = 1$ (b).

In terms of MI, the regime $|\alpha_2| > \alpha_1$ is particularly interesting, because the stability properties become intensity dependent. Since

$$\tilde{R}(k) = 0 \Rightarrow k = \pm 2\frac{\sqrt{(\sigma_1^2 - \sigma_2^2)\ln(-\alpha_1/\alpha_2)}}{\sigma_1^2 - \sigma_2^2}, \quad (14)$$

$\tilde{R}(k) \leqslant 0$ for all $k \in \mathbb{R}$ (and PWs are stable) if and only if $\sigma_1 \geqslant \sigma_2$. If $\sigma_2 > \sigma_1$, low-intensity PWs are modulationally stable, whereas high-intensity PWs are unstable. So we may have MI even though the strength of the defocusing nonlinearity exceeds that of the focusing, $|\alpha_2| > \alpha_1$. These unique stability properties are a pure consequence of the competition between nonlocal nonlinearities. In media with just one self-defocusing (self-focusing) nonlocal nonlinearity, PWs would be stable (unstable), independently of the intensity.

This intensity-dependent stability is illustrated in Fig. 3. Figure 3(a) shows the function $2\tilde{R}(k)$ together with k^2/A_0^2 vs. k for low ($A_0 = 0.5$) and high ($A_0 = 2$) intensities. We observe that for low intensity we have $k^2/A_0^2 > 2\tilde{R}(k)$ for all $k \in \mathbb{R}$, indicating stability. On the other hand, for high intensity $2\tilde{R}(k) > k^2/A_0^2$ in bounded k bands and plane waves become unstable.

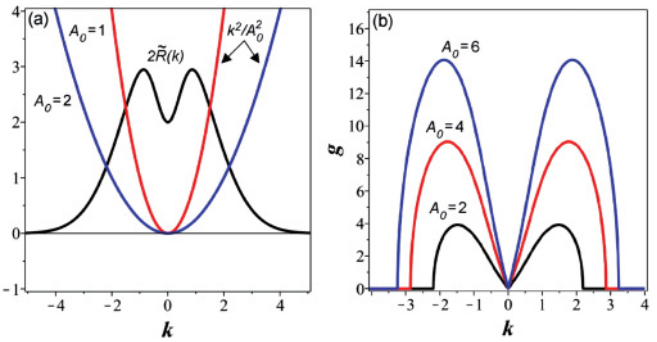

FIG. 1. (Color online) (a) Plot of the functions $2\tilde{R}(k)$ and k^2/A_0^2 for $A_0 = 1$ and $A_0 = 2$. (b) MI gain curves for $A_0 = 2$, $A_0 = 4$, and $A_0 = 6$. The medium parameters are $\alpha_1 = 2$, $\alpha_2 = -1$, $\sigma_1 = 1$, and $\sigma_2 = 3$.

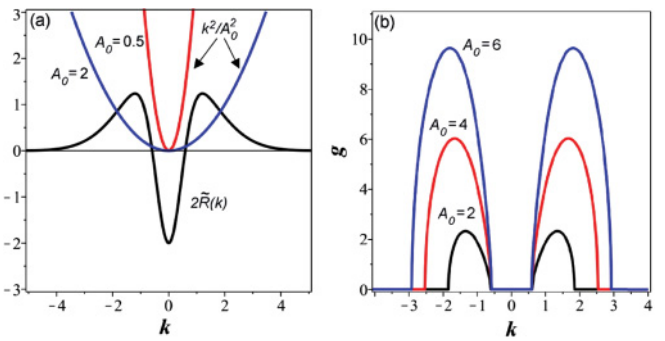

FIG. 3. (Color online) (a) Plot of the functions $2\tilde{R}(k)$ and k^2/A_0^2 when $|\alpha_2| > \alpha_1$, for $A_0 = 0.5$ and $A_0 = 2$; (b) the MI gain curves for $A_0 = 2$, $A_0 = 4$, and $A_0 = 6$. In (a) and (b) the medium parameters are $\alpha_1 = 1$, $\alpha_2 = -2$, $\sigma_1 = 1$, and $\sigma_2 = 3$.

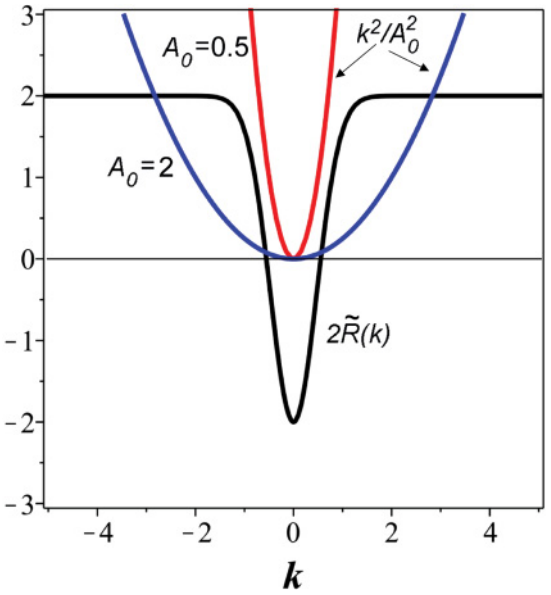

FIG. 4. (Color online) Illustrating the effect of intensity-dependent MI in case of local focusing ($\sigma_1 = 0$) and nonlocal defocusing ($\sigma_2 = 3$) competing nonlinearities. Plot of the functions $2\tilde{R}(k)$ and k^2/A_0^2 when $|\alpha_2| > \alpha_1$. Red and blue plots correspond to low ($A_0 = 0.5$) and high ($A_0 = 2$) intensity. The medium parameters are $\alpha_1 = 1, \alpha_2 = -2$.

The resulting gain curves for $A_0 = 2$, $A_0 = 4$, and $A_0 = 6$ are shown in Fig. 3(b). The maximum gain as well as the gain bandwidth increases with intensity, similarly to the case in Fig. 2(b). However, we do not have MI for sufficiently small wave numbers, meaning that small-amplitude long waves can propagate along with the background intense PWs without growing.

It is worth noting that the intensity-dependent stability of plane waves is also preserved when the focusing nonlinearity is local, i.e., $\sigma_1 = 0$. In fact, this unique stability property has been already reported in the context of Bose-Einstein condensate with simultaneous contact (local) attractive and long-range dipolar (nonlocal) repulsive interactions [42,44]. This situation is illustrated in Fig. 4. Again, it is clear that the plane wave becomes modulationally unstable only when the intensity of the plane wave is high enough. As a consequence, the medium may support formation of bright and dark solitons depending on the wave intensity.

Figure 5(a) shows the dependence of the MI gain on k and σ_1 for constant $\sigma_2 = 10$ and PW amplitude $A_0 = 1$. We observe that the maximum gain and bandwidth decreases with increasing σ_1. For sufficiently large σ_1, MI is completely suppressed. The dependence of the gain on k and σ_2 for constant $\sigma_1 = 1$ and PW amplitude $A_0 = 1$ is shown in Fig. 5(b). For small σ_2, the plane wave is modulationally stable since $k^2/A_0^2 > 2\tilde{R}(k)$ for all $k \in \mathbb{R}$. When σ_2 reaches a certain threshold value MI appears, and the maximum gain as well as the MI bandwidth increases with increasing σ_2. For sufficiently large σ_2, the maximum gain reaches an almost constant value.

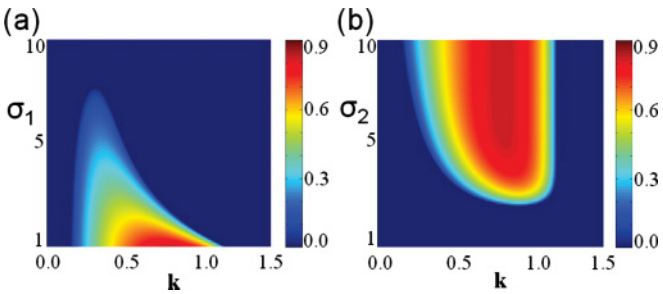

FIG. 5. (Color online) MI gain as function of wave vector k and σ_1 (a) and σ_2 (b) for $A_0 = 1$ and $|\alpha_2| > \alpha_1$. The medium parameters are $\alpha_1 = 1, \alpha_2 = -2$. In (a) $\sigma_2 = 10$ and in (b) $\sigma_1 = 1$.

IV. DYNAMICS OF MODULATIONAL INSTABILITY AND SOLITON FORMATION

To demonstrate the stability (or instability) properties of nonlocal media with competing nonlinearities we numerically "propagate" plane-wave solutions using Eq. (1) employing a split-step Fourier beam propagation scheme. As initial condition we use a PW with imposed weak periodic perturbation

$$u(x, z = 0) = A_0 [1 + \epsilon \cos(kx)], \tag{15}$$

where we assumed a relative value of the perturbation $\epsilon = 10^{-4}$.

The graphs in Fig. 6 show the evolution of the perturbed PW solution with wave number $k = 1$ and amplitude $A_0 = 1$ in case of $\sigma_1 = 1$ (a) and $\sigma_1 = 1.2$ (b). The other parameters are $\alpha_1 = 2$, $\alpha_2 = -1$, and $\sigma_2 = 3$, so we are in the regime where $\alpha_1 > |\alpha_2|$. In both figures we observe the development of MI of the PW. However, it is also evident that increasing the width of the self-focusing response σ_1 suppresses the instability by lowering the gain, as predicted by the linear stability analysis. The figures depict the normalized intensity $I(x,z)/\sup\{I(x,0) \mid x \in \mathbb{R}\}$. In the regime where $|\alpha_2| > \alpha_1$, the stability properties are predicted to be intensity dependent by the linear stability analysis. The propagation of perturbed PW solutions with perturbation wave number $k = 1$ and amplitude $A_0 = 0.85$ and $A_0 = 1.0$ is shown in Fig. 7(a) and Fig. 7(b), respectively. The medium parameters are $\alpha_1 = 1$, $\alpha_2 = -2$, $\sigma_1 = 1$, and $\sigma_2 = 3$. We observe that the low-amplitude wave is stable (note the scale on the color bar), whereas the perturbation grows with propagation when the amplitude is increased. The simulations are in agreement with the analytical results.

We mentioned earlier that bright solitons may exist when the PW solution is unstable, while the generation of dark solitons requires the absence of MI of the constant intensity

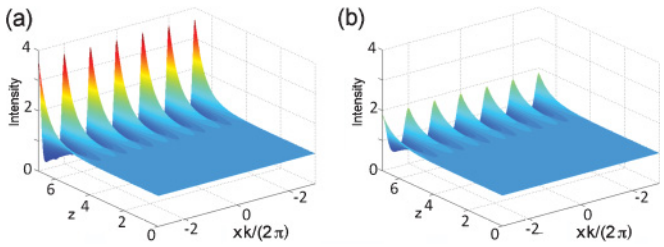

FIG. 6. (Color online) Propagation of perturbed plane wave in the regime $\alpha_1 > |\alpha_2|$ for $\sigma_1 = 1.0$ (a) and $\sigma_1 = 1.2$ (b). Plots show evolution of the normalized intensity (in arbitrary units) of the wave. In both cases $A_0 = 1$, wave number of perturbation $k = 1$, $\alpha_1 = 2$, $\alpha_2 = -1$, and $\sigma_2 = 3$.

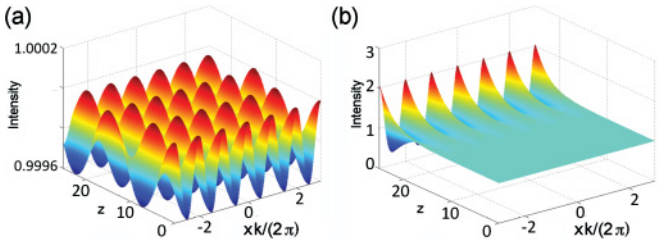

FIG. 7. (Color online) (a) Evolution of the normalized intensity of the perturbed plane wave in the regime $|\alpha_2| > \alpha_1$ and $A_0 = 0.85$. (a) Stable propagation for $A_0 = 0.85$ and development of modulational instability (b) for $A_0 = 1.0$. In both cases wave vector of the perturbation $k = 1$. The medium parameters are $\alpha_1 = 1$, $\alpha_2 = -2$, $\sigma_1 = 1$, and $\sigma_2 = 3$.

background. Since the stability properties of nonlocal media with $|\alpha_2| > \alpha_1$ are intensity dependent, one should be able to generate both bright and dark solitons in the same medium just by changing the intensity of the background wave.

In order to generate bright solitons we use the wave $u(x,z = 0) = A_0 + \mathrm{sech}(x)$ as the initial condition in Eq. (1). Figure 8 shows the propagation of waves with background amplitude $A_0 = 0.85$ and $A_0 = 1.0$. When the background intensity is too low [Fig. 8(a)] the MI does not occur, and, therefore, no bright solitons are generated. But when the intensity is increased and the background becomes unstable we observe, in Fig. 8(b), the formation of several bright solitons. The graphs in the bottom rows of this figure illustrate the corresponding input and output intensities and refractive index profiles.

In order to demonstrate generation of dark solitons in the same medium we will use the initial profile in the form $u(x,z = 0) = A_0 \tanh(x - x_0)\tanh(x + x_0)$. Such initial

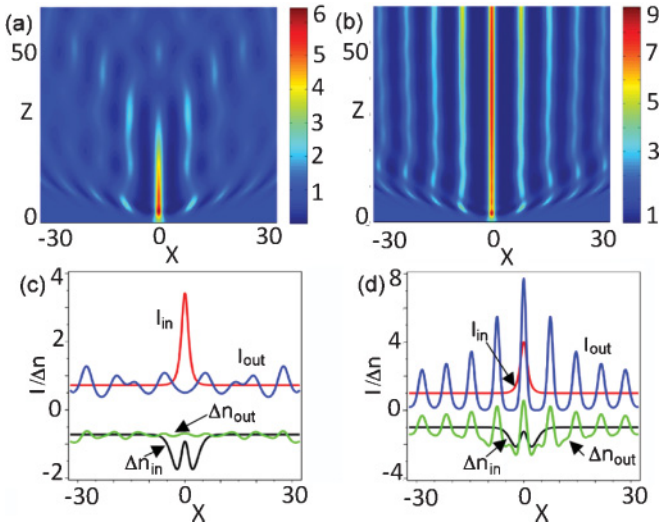

FIG. 8. (Color online) Dynamics of localized beams on infinite background in media with competing nonlocal nonlinearities. (Top row) Evolution of the beam intensity. (Bottom row) Input and output intensity (I) and refractive index profiles (Δn). Input amplitude profile $u(x,z = 0) = A_0 + \mathrm{sech}(x)$. (a) Diffraction for $A_0 = 0.85$, the background below the threshold for MI. (b) Formation of multiple bright solitons for $A_0 = 1$. The medium parameters are $\alpha_1 = 1$, $\alpha_2 = -2$, $\sigma_1 = 1$, and $\sigma_2 = 3$.

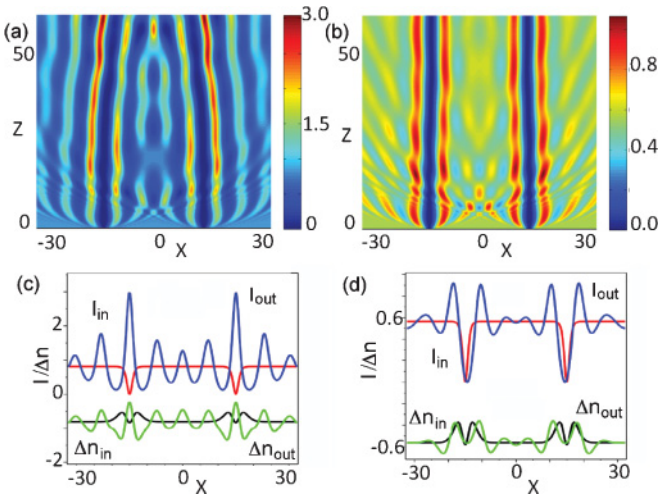

FIG. 9. (Color online) Evolution of the "dark beams" in media with competing nonlinearities from the initial amplitude distribution $u(x,z) = A\tanh(x - x_0)\tanh(x + x_0)$. (Top row) Evolution of the beam intensity. (Bottom row) Input and output intensities (I) and refractive index profiles (Δn). (a) Unstable background ($A_0 = 0.85$) and breakup of the initial structure and formation of bright solitons. (b) Stable background ($A_0 = 0.75$) and formation of two dark solitons. The medium parameters are $\alpha_1 = 1$, $\alpha_2 = -2$, $\sigma_1 = 1$, and $\sigma_2 = 3$.

conditions used in a defocusing medium results in formation of two repelling dark solitons. Figures 9(a) and 9(b) show the propagation of the wave with $x_0 = 5$ and background amplitude $A_0 = 0.85$ and $A_0 = 0.75$, respectively. When the background intensity is higher than the threshold for MI the initial amplitude distribution experiences instability and breaks up leading to the formation of bright solitons [Fig. 9(a)]. On the other hand, for sufficiently low (i.e., below the MI threshold) background intensity, the MI is suppressed and we observe in Fig. 9(b) the formation of two dark solitons. Again, the graphs in the bottom row of this figure illustrate the corresponding input and output intensities and refractive index profiles.

As the stability properties of the plane wave depends crucially on the intensity one can envisage a situation when both bright and dark solitons may coexist on the same

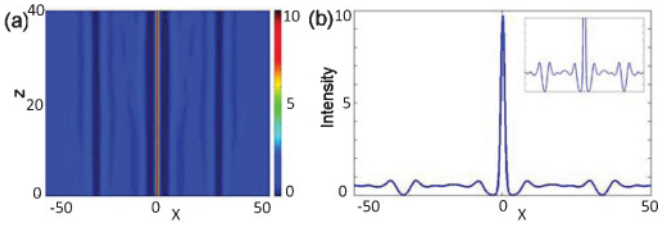

FIG. 10. (Color online) Coexistence of bright and dark solitons in media with competing nonlinearities. (a) Dynamics of soliton propagation. (b) Intensity profile of bright and dark solitons located on the same constant background. (Inset) Details of the dark solitons. The solitons have been excited using the following initial conditions: $u(x,0) = 1.911\exp[-(x/20.97)^2] - 0.72\tanh[(0.66(x - 30)])\tanh[(0.66(x + 30)]$. The medium parameters are $\alpha_1 = 1$, $\alpha_2 = -2$, $\sigma_1 = 1$, and $\sigma_2 = 3$.

background as long as its intensity is below the MI threshold. Indeed, such a situation is illustrated in Fig. 10, where we show the evolution of two dark solitons and one bright soliton. In this case, the solitons have been simultaneously excited using the initial conditions $u(x,0) = 1.911\ \exp(-x^2/20.97^2) - 0.72\ \tanh[0.66(x-30)]\tanh[0.66(x+30)]$. In fact, such initial amplitude distribution leads also to excitation of dispersive waves due to the mismatch between the initial conditions and the exact soliton profiles. In order to minimize this effect the numerical propagation was combined with application of numerical filtering which removed the excess of dispersive waves. This procedure resulted in refinement of the beam amplitude distribution so it represented more faithfully the actual soliton profiles. The refined amplitude was then used in the propagation shown in Fig. 10.

The unique medium properties observed in Figs. 8–10 are a result of the competing self-focusing and self-defocusing nonlocal Kerr nonlinearites and cannot be observed in nonlocal media with just one type of nonlinearity.

V. CONCLUSIONS

In conclusion, we analyzed conditions for the modulational instability of plane waves propagating in nonlocal nonlinear media with competing focusing and defocusing nonlinearities. We showed that presence of these nonlinear responses with different strengths and degrees of nonlocality dramatically affects the stability of plane waves. Unlike earlier works we considered here an arbitrary degree of nonlocality of both competing nonlinearities (finite σ_1 and σ_2) which allowed us to reveal that the MI, in fact, occurs only for a finite region of σ_1 values below a σ_2-dependent threshold, as seen in Fig. 5. This interesting physical effect could not be achieved with a fixed local focusing nonlinearity ($\sigma_1 = 0$) as in Refs. [42,44]. Moreover, we demonstrated that in the case when the strength of the defocusing nonlinearity is greater than that of the focusing, the stability critically depends on the wave intensity. For an intensity larger than the threshold value the plane wave is modulationally unstable and the medium supports formation of bright solitons. On the other hand, for an intensity lower than the threshold the plane wave is modulationally stable and the same medium supports formation of dark solitons. Our theoretical predictions have been confirmed by numerical simulations.

ACKNOWLEDGMENTS

This work was supported by the Australian Research Council. M.B. acknowledges support from the Danish Council for Independent Research (Project No. 274-08-0479). A.W. acknowledges the DAAD RISE program for support.

[1] *Optical Solitons - Theory and Experiment*, edited by J. R. Taylor (Cambridge University Press, 1992).
[2] Yu. S. Kivshar and G. Agrawal, *Optical Solitons: From Fibers to Photonic Crystals* (Academic Press, San Diego, 2003).
[3] W. Krolikowski, O. Bang, N. I. Nikolov, D. Neshev, J. Wyller, J. J. Rasmussen, and D. Edmundson, J. Opt. B **6**, S288 (2004).
[4] A. Snyder and J. Mitchell, Science **276**, 1538 (1997).
[5] F. W. Dabby and J. B. Whinnery, Appl. Phys. Lett. **13**, 284 (1968).
[6] S. Skupin, M. Saffman, and W. Krolikowski, Phys. Rev. Lett. **98**, 263902 (2007).
[7] D. Suter and T. Blasberg, Phys. Rev. A **48**, 4583 (1993).
[8] E. A. Ultanir, D. Michaelis, F. Lederer, and G. I. Stegeman, Opt. Lett. **28**, 251 (2003).
[9] S. Burger, K. Bongs, S. Dettmer, W. Ertmer, K. Sengstock, A. Sanpera, G. V. Shlyapnikov, and M. Lewenstein, Phys. Rev. Lett. **83**, 5198 (1999).
[10] F. Dalfovo, S. Giorgini, L. P. Pitaevski, and S. Stringari, Rev. Mod. Phys. **71**, 463 (1999).
[11] T. Lahaye, C. Menotti, L. Santos, M. Lewenstein, and T. Pfau, Rep. Prog. Phys. **72**, 126401 (2009).
[12] E. Braun, L. P. Faucheux, and A. Libchaber, Phys. Rev. A **48**, 611 (1993).
[13] G. Assanto and M. Peccianti, IEEE J. Quantum Electron. **39**, 13 (2003).
[14] C. Conti, M. Peccianti, and G. Assanto, Phys. Rev. Lett. **91**, 073901 (2003).
[15] N. I. Nikolov, D. Neshev, O. Bang, and W. Z. Krolikowski, Phys. Rev. E **68**, 036614 (2003).
[16] J. Wyller, W. Krolikowski, O. Bang, D. E. Petersen, and J. J. Rasmussen, Physica D **227**, 8 (2007).
[17] F. O. Ilday, K. Beckwitt, Y.-F. Chen, H. Lim, and F. W. Wise, J. Opt. Soc. Am. B **21**, 376 (2004).
[18] M. Bache, O. Bang, J. Moses, and F. W. Wise, Opt. Lett. **32**, 2490 (2007).
[19] M. Bache, O. Bang, W. Krolikowski, J. Moses, and F. W. Wise, Opt. Express **16**, 3273 (2008).
[20] S. K. Turitsyn, Teor. Mat. Fiz. **64**, 226 (1985).
[21] O. Bang, W. Krolikowski, J. Wyller, and J. J. Rasmussen, Phys. Rev. E **66**, 046619 (2002).
[22] D. Mihalache, D. Mazilu, F. Lederer, B. A. Malomed, Y. V. Kartashov, L.-C. Crasovan, and L. Torner, Phys. Rev. E **73**, 025601(R) (2006).
[23] D. Briedis, D. E. Petersen, D. Edmundson, W. Krolikowski, and O. Bang, Opt. Express **13**, 435 (2005).
[24] A. I. Yakimenko, Y. A. Zaliznyak, and Y. Kivshar, Phys. Rev. E **71**, 065603 (2005).
[25] Y. V. Kartashov, V. A. Vysloukh, and L. Torner, Opt. Express **15**, 9378 (2007).
[26] Y. Y. Lin, R. K. Lee, and Y. S. Kivshar, J. Opt. Soc. Am. B **25**, 576 (2008).
[27] A. Armaroli, S. Trillo, and A. Fratalocchi, Phys. Rev. A **80**, 053803 (2009).
[28] S. Skupin, O. Bang, D. Edmundson, and W. Krolikowski, Phys. Rev. E **73**, 066603 (2006).
[29] M. Peccianti, K. A. Brzdakiewicz, and G. Assanto, Opt. Lett. **27**, 1460 (2002).
[30] N. Nikolov, D. Neshev, W. Krolikowski, O. Bang, J. J. Rasmussen, and P. L. Christiansen, Opt. Lett. **29**, 286 (2004).
[31] P. D. Rasmussen, O. Bang, and W. Krolikowski, Phys. Rev. E **72**, 066611 (2005).

[32] A. Dreischuh, D. N. Neshev, D. E. Petersen, O. Bang, and W. Krolikowski, Phys. Rev. Lett. **96**, 043901 (2006).
[33] Q. Kong, Q. Wang, O. Bang, and W. Krolikowski, Phys. Rev. A **82**, 013826 (2010).
[34] J. Mitchell and A. W. Snyder, J. Opt. Soc. Am. B **16**, 236 (1999).
[35] F. W. Ye, Y. V. Kartashov, and L. Torner, Phys. Rev. A **77**, 043821 (2008).
[36] X. Hutsebaut, C. Cambournac, M. Haelterman, A. Adamski, and K. Neyts, Opt. Commun. **233**, 211 (2004).
[37] C. Rotschild, M. Segev, Z. Xu, Y. V. Kartashov, and L. Torner, Opt. Lett. **31**, 3312 (2006).
[38] W. Krolikowski, O. Bang, and J. Wyller, Phys. Rev. E **70**, 036617 (2004).
[39] O. Bang, D. Edmundson, and W. Krolikowski, Phys. Rev. Lett. **83**, 5479 (1999).
[40] M. L. Quiroga-Teixeiro and H. Michinel, J. Opt. Soc. Am. B **14**, 2004 (1997); M. L. Quiroga-Teixeiro, A. Berntson, and H. Michinel, *ibid.* **16**, 1697 (1999); I. Towers, A. V. Buryak, R. A. Sammut, B. A. Malomed, L. C. Crasovan, and D. Mihalache, Phys. Lett. A **288**, 292 (2001); B. A. Malomed, L.-C. Crasovan, and D. Mihalache, Physica D **161**, 187 (2002).
[41] J. F. Corney and O. Bang, Phys. Rev. E **64**, 047601 (2001).
[42] J. Cuevas, B. A. Malomed, P. G. Kevrekidis, and D. J. Frantzeskakis, Phys. Rev. A **79**, 053608 (2009).
[43] A. Griesmaier, J. Stuhler, T. Koch, M. Fattori, T. Pfau, and S. Giovanazzi, Phys. Rev. Lett. **97**, 250402 (2006).
[44] S. Sinha and L. Santos, Phys. Rev. Lett. **99**, 140406 (2007).
[45] L. Bergé, O. Bang, J. J. Rasmussen, and V. K. Mezentsev, Phys. Rev. E **55**, 3555 (1997).
[46] O. Bang, Y. S. Kivshar, and A. V. Buryak, Opt. Lett. **22**, 1680 (1997).
[47] M. Warenghem, J. F. Blach, and J. F. Henninot, J. Opt. Soc. Am. B **25**, 1882 (2008).
[48] I. B. Burgess, M. Peccianti, G. Assanto, and R. Morandotti, Phys. Rev. Lett. **102**, 203903 (2009).
[49] D. Mihalache, D. Mazilu, F. Lederer, L. C. Crasovan, Y. V. Kartashov, L. Torner, and B. A. Malomed, Phys. Rev. E **74**, 066614 (2006).
[50] Y. V. Kartashov, V. A. Vysloukh, and L. Torner, Phys. Rev. A **79**, 013803 (2009).
[51] Z. Xu, Y. V. Kartashov, and L. Torner, Phys. Rev. E **73**, 055601 (2006).
[52] Z. Zhou, Y. Du, C. Hou, H. Tian, and Y. Wang, J. Opt. Soc. Am. B **28**, 1583 (2011).
[53] Y. Du, Z. Zhou, H. Tian, and D. Liu, J. Opt. **13**, 015201 (2010).
[54] J. Wyller, W. Krolikowski, O. Bang, and J. J. Rasmussen, Phys. Rev. E **66**, 066615 (2002).
[55] Q. Kong, Q. Wang, O. Bang, and W. Krolikowski, Opt. Lett. **35**, 2152 (2010).
[56] W. Krolikowski, O. Bang, J. J. Rasmussen, and J. Wyller, Phys. Rev. E **64**, 016612 (2001).